CHEMICAL ENGINEERING TRANSACTIONS
VOL. 50, 2016
A publication of AIDIC
The Italian Association of Chemical Engineering
Online at www.aidic.it/cet
Guest Editors: Katharina Kohse-Höinghaus, Eliseo Ranzi

ISBN 978-88-95608-41-9; **ISSN** 2283-9216
DOI: 10.3303/CET1650027

Composition and Morphology of Ash Produced in a Waste-to-Energy (WtE) Plant

Liang Wang[a]*, Bjarte Øye[b], Michael Becidan[a], Morten Fossum[c], Øyvind Skreiberg[a]

[a]SINTEF Energy Research, Trondheim, Norway
[b]SINTEF Materials and Chemistry, Trondheim, Norway
[c]Statkraft Varme, Trondheim, Norway
liang.wang@sintef.no

In the present work, the chemical and mineralogical compositions of ashes collected from a Waste-to-Energy (WtE) plant are characterized and evaluated. The ash samples are collected vertically from bottom to top of the right side wall of the primary combustion chamber. The collected ash samples include ash slag formed in the vicinity of the grate and ash deposits formed on the boiler wall.
Ash samples are analysed via an X-ray fluorescence (XRF) spectrometer and a scanning electron microscopy equipped with energy dispersive X-ray spectroscopy (SEM-EDX), in order to obtain both bulk and micro chemical compositions. In addition, mineralogical phases in the ash samples are characterized via X-Ray powder diffraction (XRD). It is observed that the slag sample has completely melted into a dense clinker that has a clear layer structure along the thickness. XRF and SEM-EDX analyses on each layer reveal clear differences in chemical compositions and associations of the detected chemical elements. XRD analyses of ash deposits collected from different locations showed that they contain mixtures of salts, silicates and oxides formed during combustion of the MSW. However, concentrations of certain elements are different for ash deposits sampled from different locations, indicating partitioning differences during the transportation from bottom to top of the primary combustion chamber. Accordingly, proper treatment and disposing methods should be considered for the ash deposits collected from different locations in the incineration plant.

1. Introduction

Incineration is a widely implemented technology for disposal of Municipal Solid Waste (MSW), as well as energy recovery. MSW normally has a high concentration of ash forming elements. During incineration, these ash forming elements undergo complicated transformation processes and might cause ash related operational problems, mainly fouling and slagging (Lindberg et al. 2015). This will reduce heat transfer efficiency, disturb the incineration process and lead to unscheduled shutdowns of the boiler in extreme cases. Additionally, as the main residue derived from a MSW incineration process, the chemical composition of the ash is critical for further recycling, utilization or final disposal (Lindberg et al. 2015). Therefore, it is important to obtain detailed characteristics of ashes from MSW incineration plants, in order to prevent ash related operation problems and to treat the ash properly.
Many studies have been carried out in order to study ash transformation and deposits formation via experiments and thermodynamic equilibrium calculation tools (Eichelet et al. 2013; Becidan et al. 2015). Briefly, high volatility elements including alkali metals, Cl, S, Zn and Pb are rapidly released from the MSW and readily form different compounds and eutectics that have low melting temperatures. These will be transported by flue gas and condense on heat transfer tube surfaces in the cooler regions of the boiler. It leads to formation of a primary deposit layer that makes the heat transfer tube sticky. As a result of this, fly ash particles passing by will be captured on these tube surfaces, causing deposit growth. However, deposits formation mechanisms and their properties can be considerably different, as they are formed in different boilers and different sections in a boiler.
In the present work, the ash deposits were collected along the flue gas flow direction for analysing the mineralogical and chemical compositions of them. The analyses results are correlated with macroscopic

Please cite this article as: Wang L., Oye B., Becidan M., Fossum M., Skreiberg O., 2016, Composition and morphology of ash produced in a waste-to-energy (wte) plant, Chemical Engineering Transactions, 50, 157-162 DOI: 10.3303/CET1650027

appearance and microstructure/chemistry. Based on these data, ash transformation reactions and deposits formation mechanisms are discussed.

2. Experimental methods and materials

Two ash deposits and one slag sample were collected from a Waste-to-Energy (WtE) plant in Trondheim, Norway, which is owned and operated by Statkraft Varme AS. A blend of household, commercial and industry wastes are delivered by trucks and dumped into a bunker. Mixing and feeding of the waste into the combustion unit are performed by cranes. The combustion system is based on a moving grate and two-stage combustion air injection. The primary air is preheated and distributed throughout the grate in several separately controlled zones. The bottom ash is discharged to a chain conveyor. Secondary combustion is controlled by injection of both air and recirculated flue gas. Heat recovery is achieved by a hot water boiler system with an entry gas temperature of 750°C and exit gas temperature of 160°C. The flue gas treatment is based on a semi-dry cleaning system with no water effluents.
The two deposits analysed in this study were collected vertically from bottom to top of the right side wall of the primary combustion chamber. The ash deposit #1 was collected at a position that is 10 meters above the grate. The ash deposit #2 was collected from the top of the combustion chamber, where the flue gas turns and flows into the superheater section. The slag sample was collected from the right side wall (looking from the feeding system) about 1.5 meters above the grate. This means that the sample was most probably exposed directly to flames and temperatures well above 1000°C.
The collected deposit and slag samples were firstly photographed and labelled. The deposit samples were then crushed into fine powders for further chemical and mineralogical composition determination. The deposit samples were analysed by an X-ray fluorescence (XRF) analyser (Bruker, S8 Tiger) for quantifying concentrations of main elements in a sample, which are presented on oxides form. Mineral phases in a sample were identified by an X-ray diffractometer (Bruker, D8 Advance) equipped with a Cu k-alpha radiation and LynxEye detector. Semi-quantitative analyses were performed for collected data by using the evaluation program TOPAS plus with the ICDD-PDF2 database. The morphology and microchemistry of the samples were examined by scanning electron microscopy (SEM) coupled with energy dispersive X-ray analysis (EDX). The SEM was operated to take backscattered electron images for illustrating elemental distribution in a scanned area.

3. Results and discussion

3.1 General appearance and structure of the deposit and slag sample

Figure 1 shows photos of the ash deposit #1 collected from a sampling point that is on the combustion chamber wall 10 meters above the grate. In general, the deposit sample contains mainly coarse particles, agglomerates and lumps. The latter can be broken by bare hands. No materials with clear molten appearance are observed. Compared to the ash deposit #1, a large amount of finer particles can be found in the ash deposit #2 (Figure 2(a)). However, the amount of agglomerates and lumps in the ash deposit #2 is higher than that in the ash deposit #1, as shown in Figure 2(a). Some of the lumps have a clear layered structure and curved shape as displayed in Figure 2(b), which are not found in the ash deposit #1. In addition, there are many small agglomerates and pieces with dark red colour in the ash deposit #2, indicating high content of metals in them.

(a) (b)

Figure 1: (a) general view of deposit sample #1; (b) close view of some coarse lumps.

(a) (b)

Figure 2: (a) general view of deposit sample #2; (b) close view of some coarse lumps with curved shape and layered structure.

(a) (b) (c)

Figure 3: Photos of slag sample (a) top-down view; (b) left side view; (c) front side view.

Figure 3 shows the slag collected from the sampling point 1.5 meters above the grate. The slag mainly contains totally fused material with a dense structure, which is hard and heavy as a stone. Figure 3(a) shows the intact surface of the slag which was attached to the wall. Figure 3(b) and (c) display the layer structure of the slag. The layers are characterized by different colours, implying different compositions of them. In addition, there are many voids with round and smooth rims in the slag as shown in Figure 3(b) and (c). These voids are probably formed due to release of gases from the slag as it was passing a molten stage and behaving like liquid (Phonegphiphat et al. 2011). It is interesting to see that between two layers, many coarse particles can be found. They might be ash residues transferred by the gas flow from the ash bed, which are stuck on and/or trapped in the molten slag.

3.2 Chemical and mineralogical analysis

Figure 4 displays the chemical compositions of the ash deposit #1 and #2. The ash deposit #1, collected from the lower section of the combustion chamber, contains significantly high contents of Ca, Si, Al and Fe. These elements are non- or less volatile elements in the MSW. Detection of them in the ash deposit #1 is probably due to entrainment of ash particles from the bed, which accumulate and agglomerate on the combustion chamber wall, leading to formation of a deposit layer (Phonegphiphat et al. 2010). It partially explains poor hardness and coarse macroscopic appearance of the ash deposit #1. In comparison to ash deposit #1, the contents of S, K, Na and Cl in the ash deposit #2 are significantly higher. These four elements are highly volatile and readily release during combustion of the MSW to form vapours, fine particles and/or aerosols (Becidan et al. 2009). These aerosols and fine particles will be carried out by flue gas from the bottom to the top section of the combustion chamber. As the flue gas enters the superheater tube section, these fine particles and aerosols condense on colder tube surfaces. It is also worth to mention that concentrations of minor elements in the ash deposit #1 and #2 are also different. Some elements including Br, Co, Cd and Mn are only detected in the ash deposit #2. On the other hand, V and Nb are only detected in the ash deposit #1. Such concentration differences of minor elements are mainly attributed to different volatility of these elements and consequent transformation reactions of them (Eichelet et al. 2013). Currently, the fly ash from MSW incineration plants is mostly landfilled. Fly ash fractions from the various sections of the combustion chamber and boiler should be treated differently, considering concentrations of these minor elements and distribution of them in these fly ash fractions. However, the small amounts of fly ash produced make these differentiated treatments difficult.

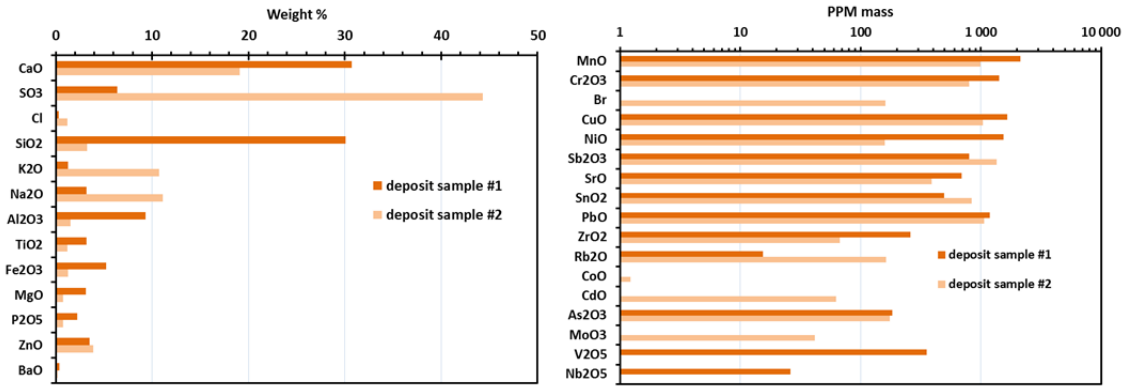

(a) (b)

Figure 4: Chemical composition of deposit sample #1 and #2 (a) main elements; (b) minor elements.

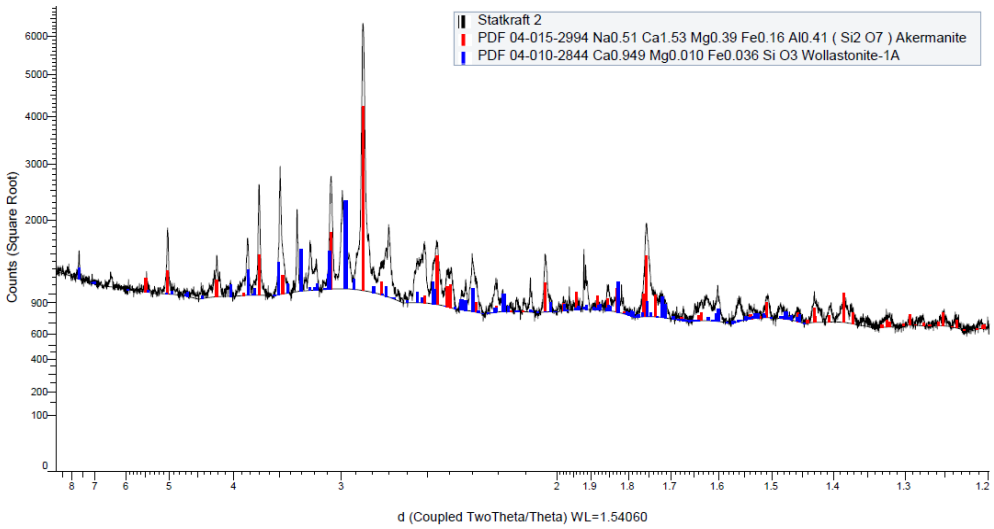

Figure 5: Mineralogical composition of deposit sample #1.

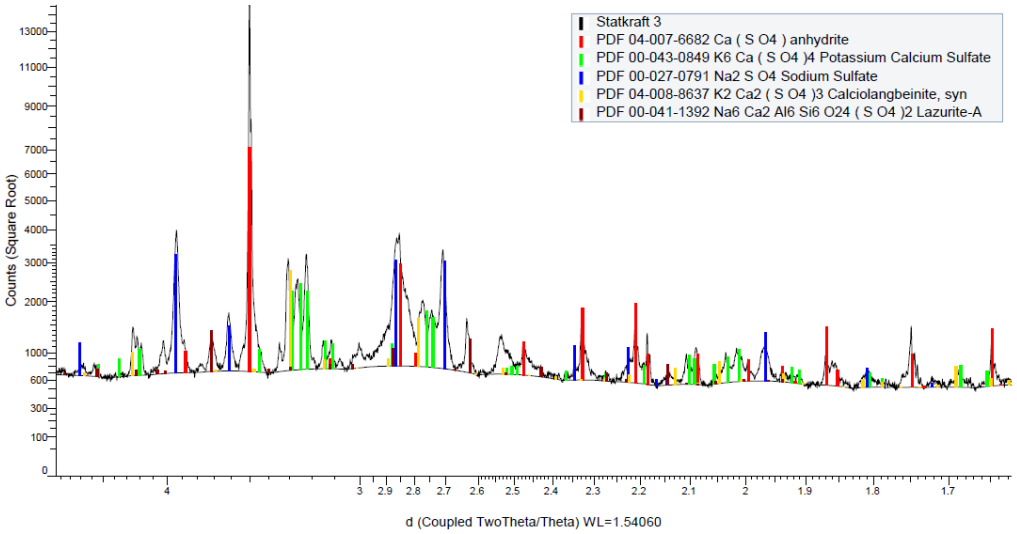

Figure 6: Mineralogical composition of deposit sample #2.

Figure 5 shows an XRD spectrum of the ash deposit #1. Akermanite (Na-Ca-Mg-Al-silicate) and wollastonite ($CaSiO_3$ with certain contents of Fe and Mg) are detected as two major mineral phases in the ash deposit #1. Compared to the ash deposits #1, a completely different mineralogical composition in the ash deposit #2 is detected (Figure 6). The ash deposits #2 contains mainly calcium sulphate, sodium sulphate and potassium calcium sulphates. The result of the XRD analysis on ash deposit #2 agrees well with XRF analysis, where alkali metals and sulphur are the main elements detected. It also confirms that release and transformation of volatile S and alkali metals is the main cause of deposits formation on heat transfer tube surfaces in the top section of the combustion chamber.

3.3 SEM-EDX analysis

Figure 7 shows a SEM image of ash deposit #1 and #2. The SEM is operated with similar operation parameters (i.e., working distance and magnification) as shown in bottom of the Figure 7(a) and (b). Therefore, it is possible to directly compare size and morphology of the scanned ash deposit #1 and #2 as they are shown in Figure 7(a) and (b). It can clearly be seen that the ash deposit #1 (Figure 7(a)) contains large agglomerates and coarse particles. On the other hand, more discrete particles can be found in the ash deposit #2 (Figure 7(b)), which generally have sizes smaller than those in Figure 7(a). Additionally, the agglomerates in Figure 7(b) have smaller sizes and more dense structure. The microscale examinations done by SEM agree well with the macroscopic observation that the ash deposit #1 contains larger and coarser particles and aggregates than the ash deposit #2.

Considering severer sintering of the deposit #2, it has been examined with more detailed SEM-EDX analyses. Figure 8(a) shows another SEM image of the ash deposit #2 that mainly contains aggregates and separated particles with irregular and spherical shapes. Figure 8(b) displays a zoom in view of the area marked with a rectangle in Figure 8(a). There are many spherical particles with different sizes. According to EDX analysis, the large round particle contains mainly SiO_2, and sinters together with other smaller particles and grains. Elements Ca and S are two dominant elements detected in those small spherical particles. They are probably molten $CaSO_4$ that condense as droplets in the deposit structure. There are also some plate-like grains shown in Figure 8(b), which is $CaSO_4$ eutectic as indicated by EDX analyses. In addition, as shown in Figure 8(b), many spherical and plate-like particles are sticking on or embedded in the molten structure that has a smooth surface, and which are rich in Ca, K, Na, Cl and S. Therefore, this molten fraction might be an eutectic of sulphates and chlorides, which have even lower melting temperatures than the parental phases (Eichelet et al. 2013). Figure 9 displays a SEM image of a small scanned area of the slag sample. EDX analyses reveal that the main elements detected in the scanned area are Ca, Si and Al, together with a small amount of alkali metals. It implies that the bulk of the slag is formed due to generation of silicates that fuse as they are exposed to the high temperature combustion zone.

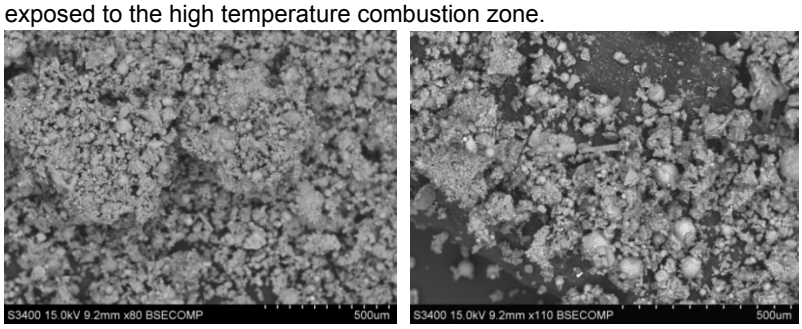

(a) (b)

Figure 7: SEM image of (a) deposit sample #1, (b) deposit sample #2.

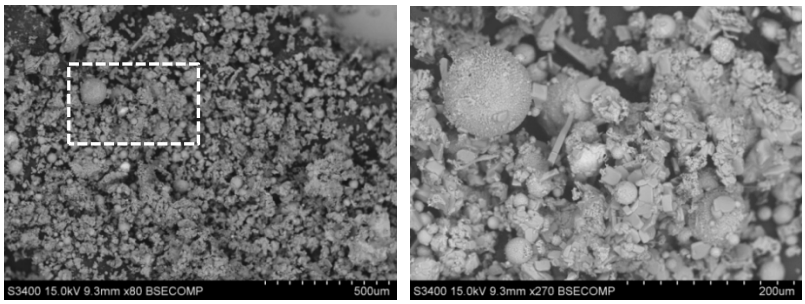

(a) (b)

Figure 8: SEM image of (a) deposit sample #2, (b) close view of selected area in (a).

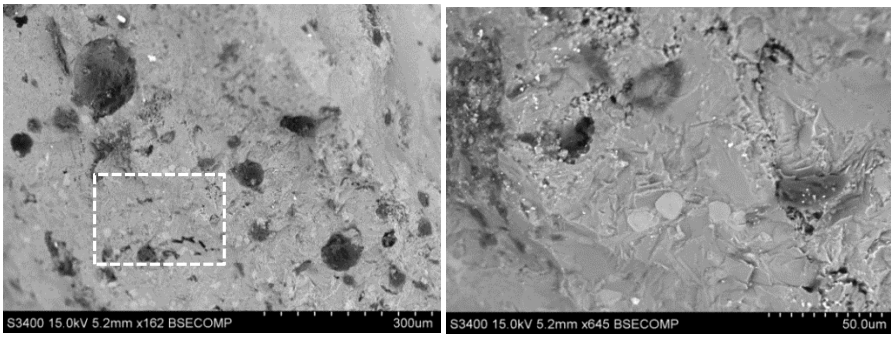

(a) (b)

Figure 9: SEM image of (a) slag sample, (b) close view of selected area in (a).

4. Conclusions

Two ash deposit samples and one slag sample were collected from a WtE plant. The macroscopic appearance and microstructure of the three samples were evaluated. The results show that, compared to the ash deposit #1 collected from the lower section of the combustion chamber, the ash deposit #2 collected at the top of the combustion chamber contains more fine particles and molten phases. The chemical and mineralogical compositions of the three samples were determined by XRF and XRD analysis, respectively. The ash deposit #2 is rich in Ca, S, Cl and alkali metals, while the ash deposit #1 contains mainly non- and less volatile Si, Ca, Al and Fe. Differences in chemical compositions of the two deposit samples are mainly related to different elemental transformations, partitioning and chemical reactions of ash forming elements in the MSW. XRD analyses show that the ash deposit #1 contains mainly akermanite and wollastonite, while the ash deposit #2 is rich in sulphates. SEM-EDX analyses agree well with the XRF and XRD analysis results. The ash deposit #2 is formed due to condensation, agglomeration and sintering of sulphates, which are rich in Ca, S, Cl and alkali metals. Formation of the ash deposit #1 is attributed to accumulation and aggregation of rather large particles containing high temperature materials. Finally, the slag sample collected close to the grate has a dense and layered structure, which is formed due to formation, accumulation and melting of silicates.

Acknowledgments

This publication has been funded by CenBio – Bioenergy Innovation Centre. CenBio is co-funded by the Research Council of Norway (193817/E20) under the FME scheme and the research and industry partners.

Reference

Becidan M., Wang L., Fossum M., Midtbust, H.O., Stuen, J., Bakken J.I. Evensen E., 2015, Norwegian Waste-to-Energy (WtE) in 2030: Challenges and Opportunities. Chemical Engineering Transactions, 43, 2401-2406.

Becidan M; Houshfar, E; Wang L., Lundstrøm P., Grimshaw A., 2015, S-Cl-Na-K chemistry during MSW gasification: A thermodynamic study. Chemical Engineering Transactions, 43, 2011-2016, DOI: 10.3303/CET1543336

Becidan, M., Sørum L., Frandsen F. Pedersen A J., 2009. Corrosion in waste-fired boilers: A thermodynamic study. Fuel, 88, 595-604.

Eichelet, J., Pfrang-Stotz, G., Bergfeldt, B., Seifert, H., Knapp, P. 2013. Formation of deposits on the surfaces of superheaters and economisers of MSW incinerator plants. Waste Management, 33, 43-51.

Lindberg D., Molin C. Hupa, M. 2015. Thermal treatment of solid residues from WtE units: A review. Waste Management, 37, 82-94.

Phonegphiphat A., Ryu C., Finney, K.N., Sharifi V.N., Swithenbank J. 2011. Ash deposit characterisation in a large-scale municipal waste-to-energy incineration plant. Journal of Hazardous Materials, 186, 218-226

Phonegphiphat A., Ryu C., Yang, Y. B., Finney, K.N., Leuland, A., Sharifi V.N., Swithenbank J. 2010. Investigation into high-temperature corrosion in a large-scale municipal waste-to-energy plant. Corrosion Science, 52, 3861-3874.